

Petrographic investigation of granites from the Metro stations in Copenhagen

Investigation of granite panel discolouring in the Metro entrance constructions, based on petrological analysis and testing porosity and permeability properties

Stig A. Schack Pedersen, Sandra Piazzolo,
Christian Høier and Niels Springer



Petrographic investigation of granites from the Metro stations in Copenhagen

Investigation of granite panel discolouring in the
Metro entrance constructions, based on
petrological analysis and testing
porosity and permeability
properties

Stig A. Schack Pedersen, Sandra Piazzolo,
Christian Høier and Niels Springer

Contents

Introduction	2
Petrographic investigation	3
General remarks:	4
Granite from Kongens Nytorv	4
Granite panel with discolouring: Kina1	4
Scanning electron microscope investigations.....	9
Granite panel without discolouring: Kina2	16
Scanning electron microscope investigations.....	19
Granite from Frederiksberg Metro Station	24
Granite from Nørreport Station	29
SEM analyses and description	32
Summary of petrography	34
Discussion of discolouring of the granite	35
Porosity and permeability tests of granite tiles	37
Summary of porosity and permeability measurements	38
Analytical Methods.....	39
Sampling	39
He-porosity and grain density	39
Liquid permeability	39
Precision of analytical data	39
Discussion of the properties of granites	40
Conclusion	41

Executive Summary

Miscoloured Chinese Granite (Samples from Kongens Nytorv and Frederiksberg Stations)

1. Fine to medium grained stone
2. Texture of stone is anisotropic i.e. shows a preferred orientation of minerals
3. Abundant fine grained, iron rich minerals (biotite and chlorite) within matrix of stone which show an irregular surface and “edged, open” grain boundaries
4. Chlorine presence within biotite and chlorite
5. High porosity and permeability relative to the reference Finnish granite from Nørreport
6. Miscolouration due to ferrous elements from within the stone oxidizing (rusting) on the surface of the cladding. Causes:
 - Fine grained, rough edged, iron rich minerals provide large surface area to be eroded by weathering elements (water and/or pollutants)
 - High porosity/permeability and anisotropy of stone provides easy access to weathering elements within the matrix of the stone – ferrous elements released within the stone’s matrix
 - Chlorine presence may accelerate release of ferrous elements within stone
 - High porosity/permeability allows transportation of released ferrous elements to the stone surface where they oxidize
7. Magnetite particles do not appear to be eroded, which would question Comet’s assertions that the magnetite is the source of the oxidizing ferrous elements

Non-miscoloured Chinese Granite (Sample from Kongens Nytorv Station)

1. Coarse grained stone
2. Texture of stone is largely isotropic i.e. shows no preferred orientation of minerals
3. Smooth surfaced biotite and chlorite with “closed” grain boundaries in stone providing reduced surface area for erosion and pathways for fluid
4. Lower porosity/permeability
5. Combination of reduced porosity/permeability and reduced surface areas of biotite/chlorite to be eroded, lower risks of ferrous elements being transported to stone surface where they would oxidize

Non-miscoloured Finnish Granite (Sample from Nørreport Station)

1. Coarse grained stone
2. Texture of stone is isotropic i.e. shows no a preferred orientation of minerals
3. Low quantities of ferrous containing biotite and chlorite with “closed” grain boundaries
4. Very low porosity/permeability
5. Low ferrous/chlorine amounts, very low porosity/permeability as well as reduced surface area of the matrix minerals make the transportation of ferrous elements to surface highly unlikely.

Introduction

Medio January 2002 the Geological Survey of Denmark and Greenland, GEUS, was asked by Ørestadsselskabet I/S (ref.: Jesper Brink Malmkjær) to inspect the discoloured granite tiles in the walls of the new build Metro Stations in Copenhagen. During this inspection three stations were visited.

At Frederiksberg, GEUS was shown cladding with the following features:

- Dark shadowing at exterior stairs which would appear to correspond to moisture penetration
- Shadowing on granite corresponding to backfill locations in interior dry locations. Similarly a removed tile from this station (later tested as sample FK) showed a direct relationship between a casting break in the backfill and the shadowing on the granite.
- Dark staining observed at some mounting location corresponding to mounting adhesives
- Yellowing of granite at the mounting locations only (not entire panel)

At Kongens Nytorv:

- Dark shadowing was observed that would seem to indicate moisture penetration
- Distinct full panel yellowing whereas adjacent panel maintained grey colour. Two panels were chosen for removal (Samples KK1 and KK2)

At Lergravsparken

- Dark shadowing was observed that would seem to indicate moisture penetration
- Limited number of yellow tiles
- Dark spots corresponding to mounting adhesive were observed
- White spots corresponding to mounting adhesive were observed

GEUS was asked to perform an investigation of the granite to determine if any of the observed conditions could be explained geologically. All of the observations indicated significant passage of materials/fluids through the stone and GEUS recommended porosity/permeability tests be included as a part of the study.

Petrographic investigation

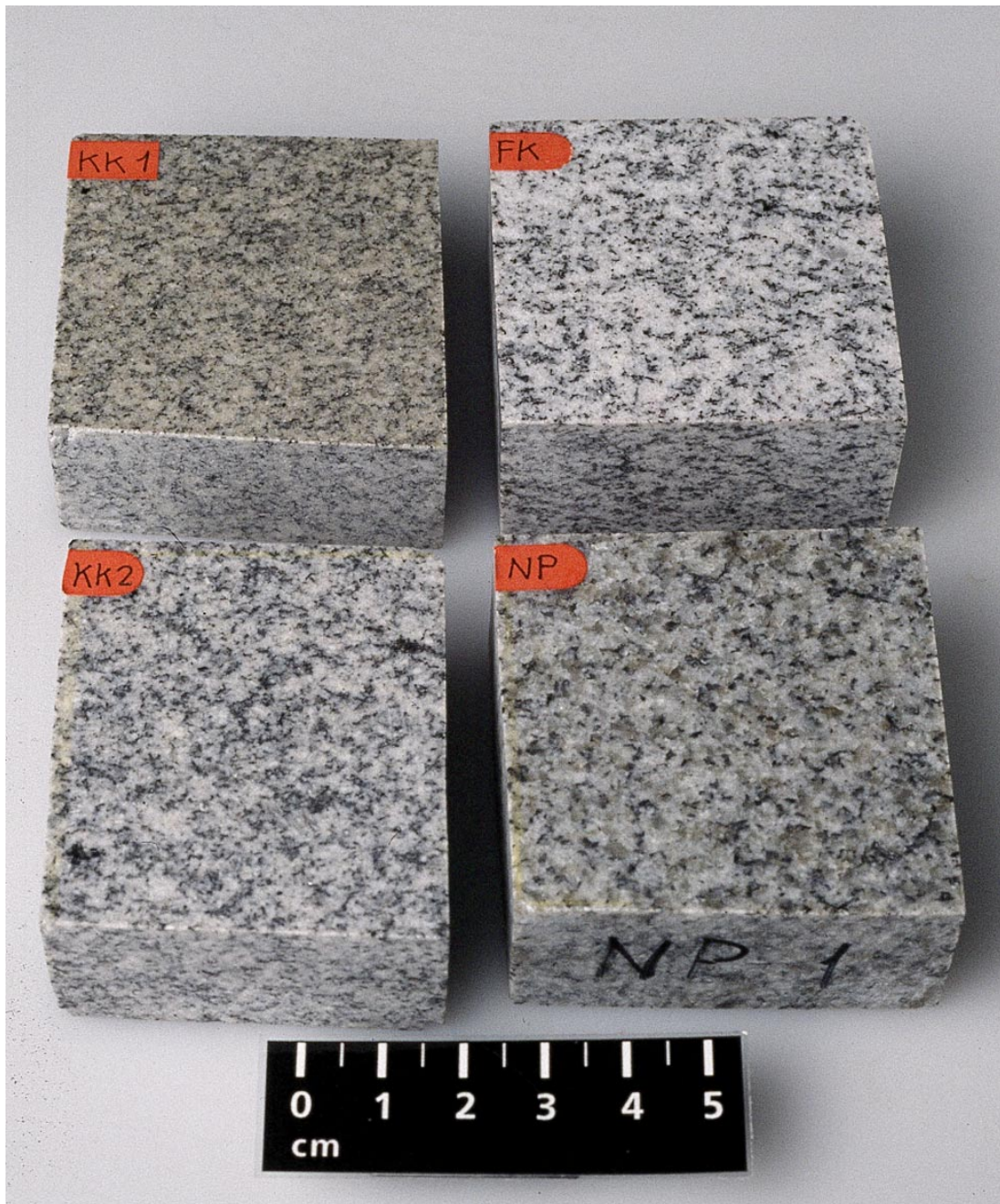


Figure 1. The four granites investigated in this report. KK1 in upper left corner is the most discoloured from Metro station Kongens Nytorv, KK2 in the lower left corner is a non-discoloured granite also from Kongens Nytorv, FK in the upper right corner is from the Metro station Frederiksber, and NP is a granites from the Metro station Nørreport.

General remarks:

Four different samples were characterised and examined in detail. These are:

- 1a) Kina1 (KK1): Granite (Chinese) from Kongens Nytorv Station exhibiting discoloration
- 1b) Kina2 (KK2): Granite (Chinese) from Kongens Nytorv Station without discoloration
- 2) FK: Granite (Chinese) from Frederiksberg Station which is partly discoloured
- 3) NP1: Granite (Finnish) from Nørreport Station which does NOT exhibit discoloration

From each of the samples several petrographic thinsections (thickness 30 µm) were prepared. The orientation of the different thinsections is shown in Figure 2. From samples Kina1, Kina2 and NP1 (see also Fig. 2), small block pieces with a honed top surface were obtained and their surface analysed in the SEM (Scanning Electron Microscope).

In the following characterisations are based on petrographic microscopy of the different samples with additional description of some details obtained from the electron microscopy.

Note that if a whole rock panel is examined, a geologist can readily determine if a rock carries a preferred orientation or no preferred orientation i.e. an alignment or non-alignment of specific minerals such as biotite and feldspar. But, an unequivocal, convincing representation of such features in form of photos of relatively small rock samples (e.g. several cm size) is difficult as both the three-dimensionality and the alignment of crystals are difficult to see in a static photograph.

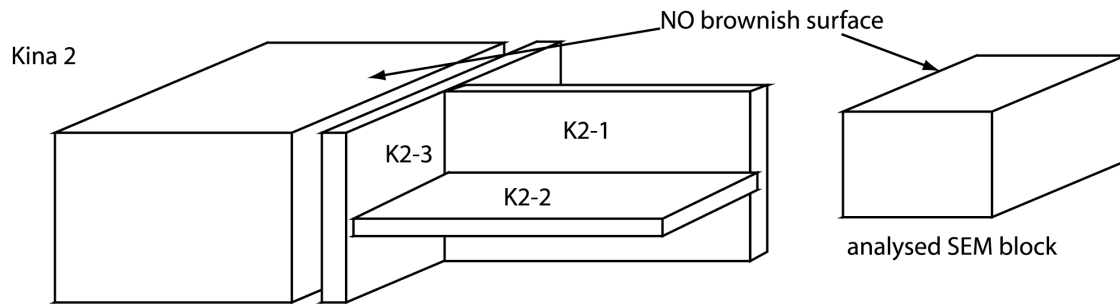
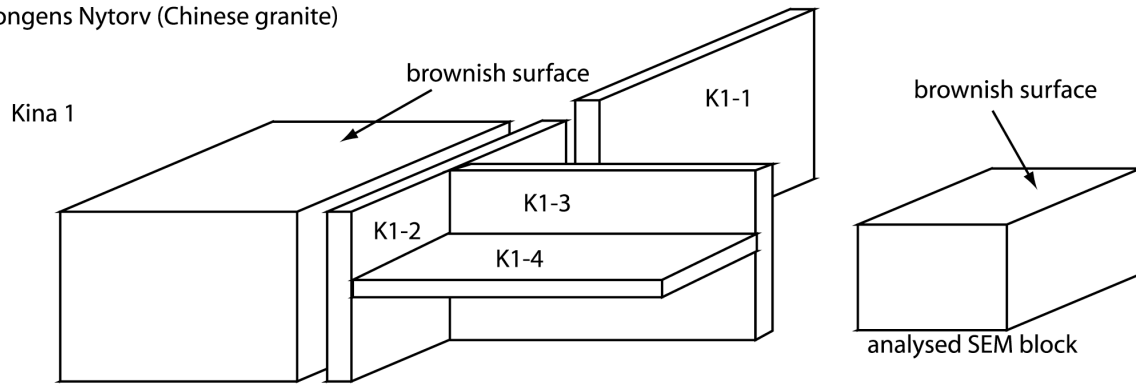
Granite from Kongens Nytorv

Granite panel with discolouring: Kina1

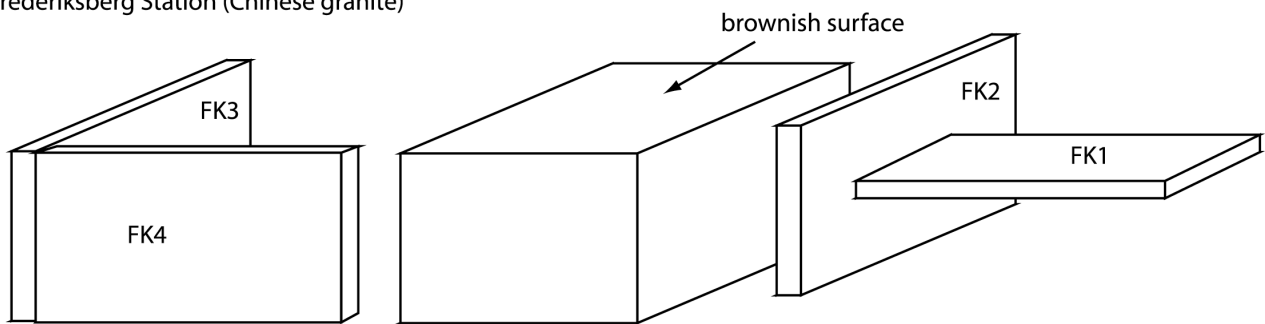
Macroscopic description:

The panel shows a noticeable fabric (Fig. 3) which is defined by planar and linear alignment of mica laths. Some alignment of Fsp laths is also present. The rock is medium grained (grain size mostly between 0.3 and 2.5 mm) and exhibits an igneous texture (Figure 12). The main constituents of the rock are quartz, feldspar and biotite, accessories are chlorite, magnetite and muscovite. Chlorite is frequently associated with magnetite or partly replaces biotite (for details see below). Magnetite crystals (0.1 – 0.5 mm) are idiomorphic and often associated with biotite and chlorite. Feldspar (up to 2.5 mm) is characterized by a chemical zonation from core to rim which is typical for feldspars of igneous origin. In addition, sericite and muscovite laths that are aligned along crystallographic planes are abundant in the core of the feldspar crystals.

Kongens Nytorv (Chinese granite)



Frederiksberg Station (Chinese granite)



Nørreport Station (Finish Granit)

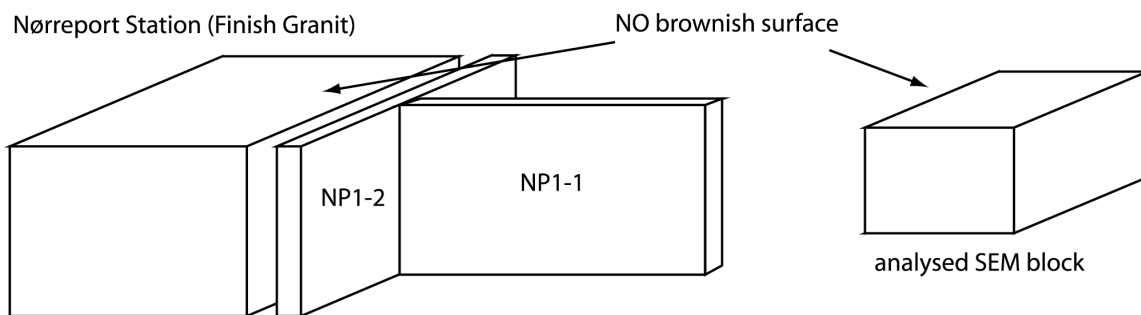


Figure 2. Sketch of the orientation of the different thinsections obtained from the investigated granite samples.



Figure 3. *Cut-out hand specimen of sample Kina1, granite from Kongens Nytorv Metro Station. Note the discoloration on the top surface and the foliated and lineated appearance of the rock.*

Microscopic description:

The general appearance of the thinsections which were cut at different orientation to the surface and fabric are shown in Figure 2. These show also the preferred orientation of biotite and chlorite in this sample (e.g. Kina1-4).

The rock exhibits two nearly perpendicular preferred orientations of the biotite (< 1 mm), feldspar and chlorite laths (Fig. 4, Fig. 5), which gives the rock the foliated and lineated appearance in hand specimen (Fig. 3). This alignment is not associated with substantial recrystallization of quartz, feldspar or biotite and is therefore interpreted to originate from syn-magmatic deformation of the crystal mesh.

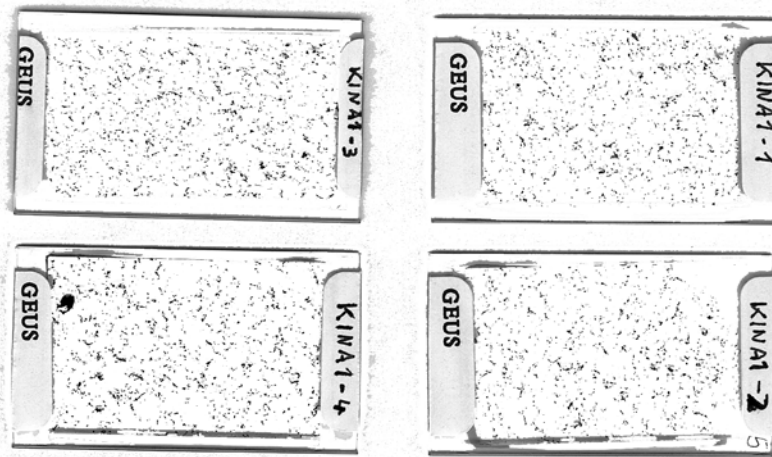


Figure 4. Scans of the 4 different thinsections made from sample Kina1. Note the shape preferred orientation of biotite in thinsections Kina1-2 and Kina1-4. For orientation of thinsections see Fig. 2. The length of the slides is ca. 5 cm.

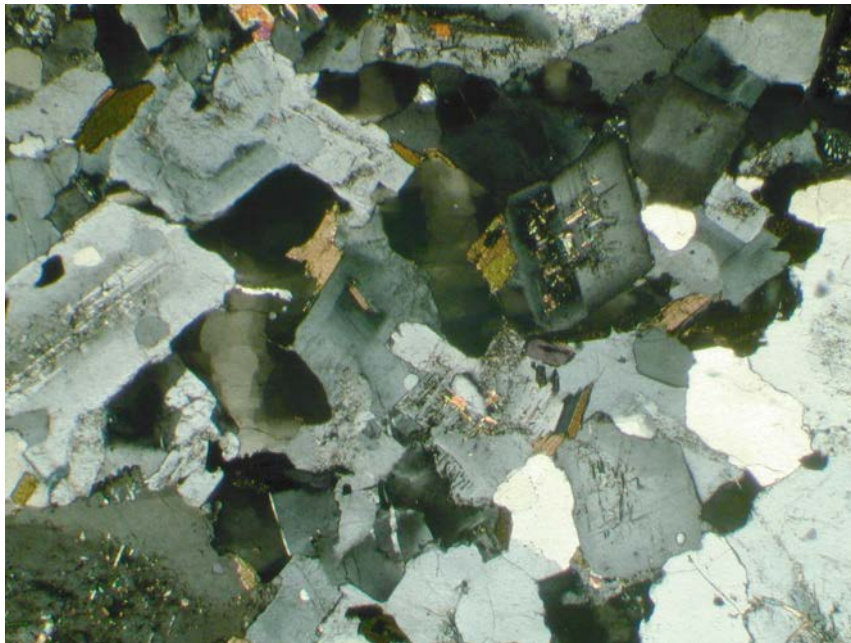


Figure 5. General appearance of Kina1 (thinsection Kina1-3) under the microscope. The igneous feldspar shows a well developed chemical zonation from core to rim and sericite/muscovite laths in the core. Quartz shows some undulatory extinction pointing to minor amount of deformation. Grain boundaries are slightly curved to straight. Micrograph is taken with crossed nicols and width of view is 6 mm.

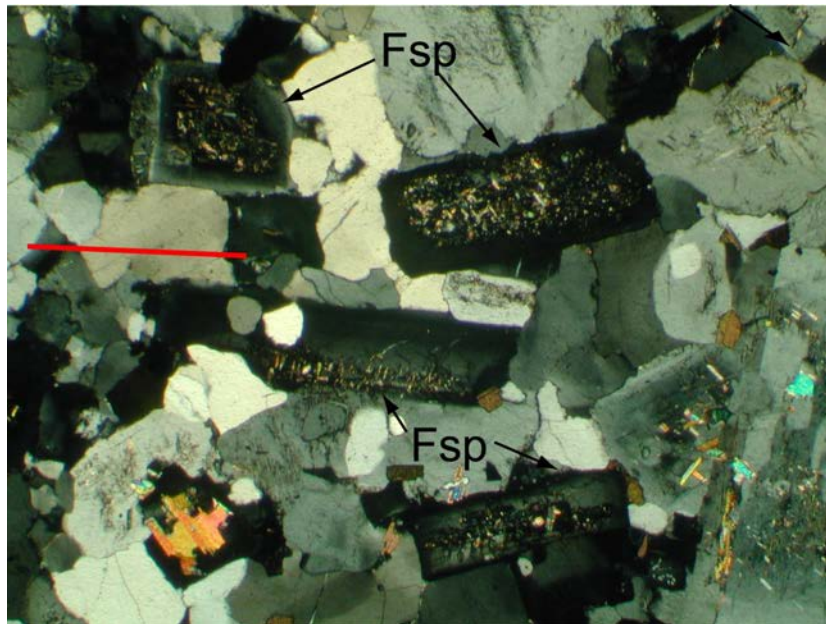


Figure 6. Preferred orientation of feldspar laths seen in Kina1-2. The red line shows the general preferred orientation and the arrows point to igneous feldspars, which are aligned. Note that alignment of igneous feldspars without recrystallization of neither feldspars nor quartz point to a igneous origin of the preferred orientation, hence synmagmatic deformation. Micrograph is taken with crossed nicols and width of view is 6 mm.

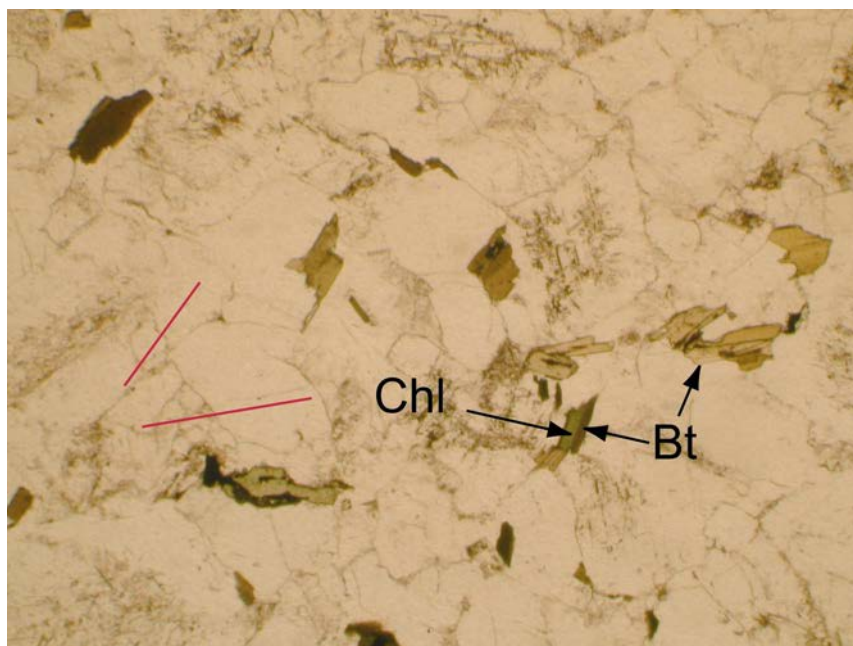


Figure 7. Photomicrograph showing the alignment of biotite and chlorite in two nearly perpendicular directions (general orientations shown in red) seen in Kina1 (thinsection Kina1-3). One of these directions corresponds to the preferred orientation of feldspar crystals as shown in Fig. 6. Note also the partial replacement of biotite by chlorite. Field of view same as above. Micrograph is taken in plain light and width of view is 6 mm.

Scanning electron microscope investigations

SEM investigations show that chlorite replaces biotite in several instances (Fig. 8 and 9). The surface of the biotite and chlorite is generally rough. The crystallographic basal <a> planes of biotite are well seen in the SE and BSE images. Chlorite has irregular surface appearance with some ditches. It seems to be of slightly lower relief than the biotite and feldspar. Grain boundaries in the vicinity of biotite-chlorite aggregates are characterized by indentations in the SE images (Fig. 9). They are "eroded". The surface of feldspars is generally smooth except for systematic ditches due to the mechanical smoothing of the surface. This is also true for the inclosed muscovite and sericite (Fig. 8 and 9). Magnetite shows idiomorphic shapes and its surface of it is characterised by shallow, concave, bowl-shaped ditches (Fig. 15) typical for mechanical working.

Examples of the composition of chlorite, biotite and feldspar are given in Tab. 1. Biotite and chlorite are Fe-rich and show some traces of Cl⁻ which replaces the OH⁻ groups in these two minerals. The feldspars are kalifeldspars or albites. The element spectrum obtained from a quartz shows not only an element peaks at Si but also distinct peaks at S, Cl, Na, K and Fe (Fig. 16).

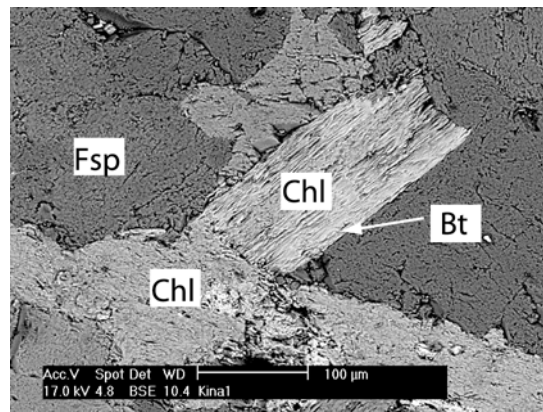


Figure 8. Chlorite replacing biotite; BSE image

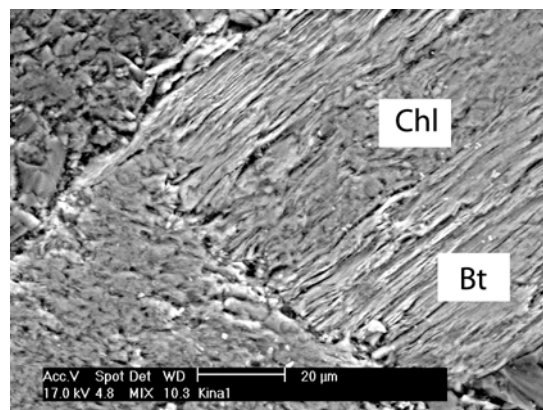


Figure 9. Close-up of Fig. 8 showing a combined image generated by a combination of a backscatter electron (showing chemical differences) and secondary electron image (showing surface structure).

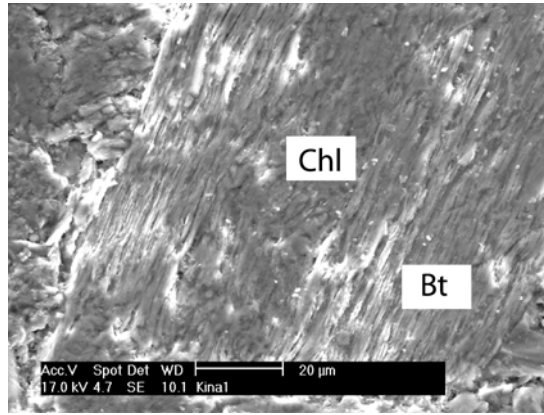


Figure 10. Similar close-up as Fig. 9; SE image showing exclusively surface structure. Note that the cleavage of biotite gives a high surface-ditch appearance to the biotite. The chlorite has an irregular surface that is generally slightly lower than the biotite and feldspar (light grey) surface.

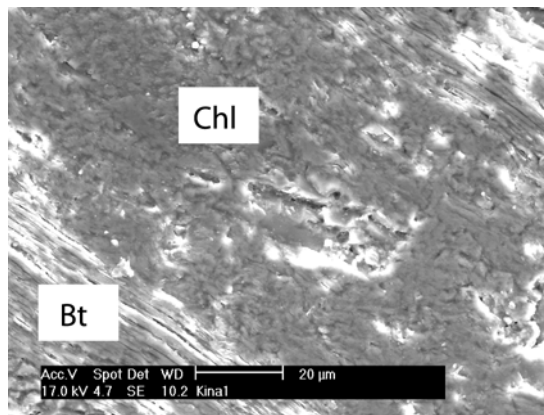


Figure 11. Close-up of another location of a biotite-chlorite aggregate; SE image. Note the ditches in both biotite and chlorite.

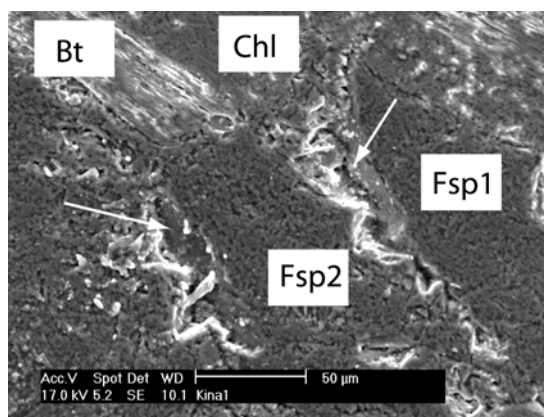


Figure 12. SE image showing the surface structure of a feldspar-feldspar boundary in the vicinity of a biotite-chlorite aggregate. Note the deep pits (arrows) along the the grain boundaries which point to severe dissolution, "erosion" along these boundaries.

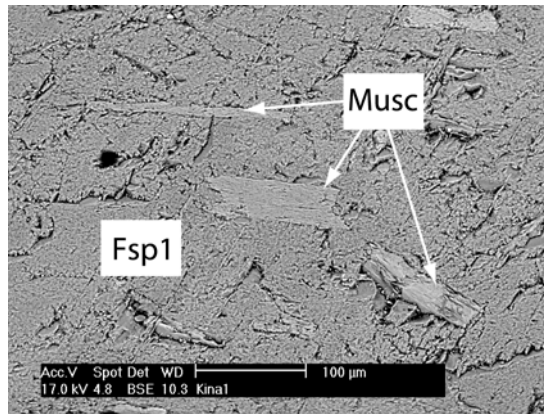


Figure 13. *Muscovite laths in feldspar; BSE image.*

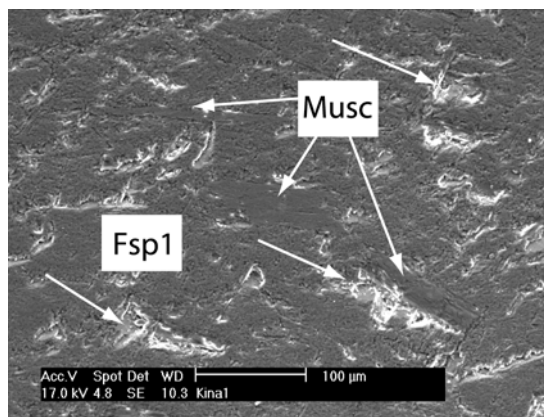


Figure 14. *Same location as Fig. 13. SE image. Note the smooth surface of feldspar and muscovite. The ditches seen are orientated in the same direction (arrows). Therefore, these pits are most likely due to the mechanical working of the surface.*

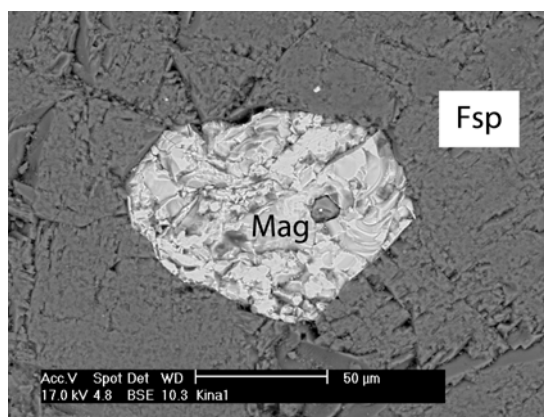


Figure 15. *Magnetite imbedded in feldspar; BSE image. The curved shapes at the upper left part of the magnetite are due to mechanical working on the surface of the magnetite. No alteration of the magnetite is seen in this image.*

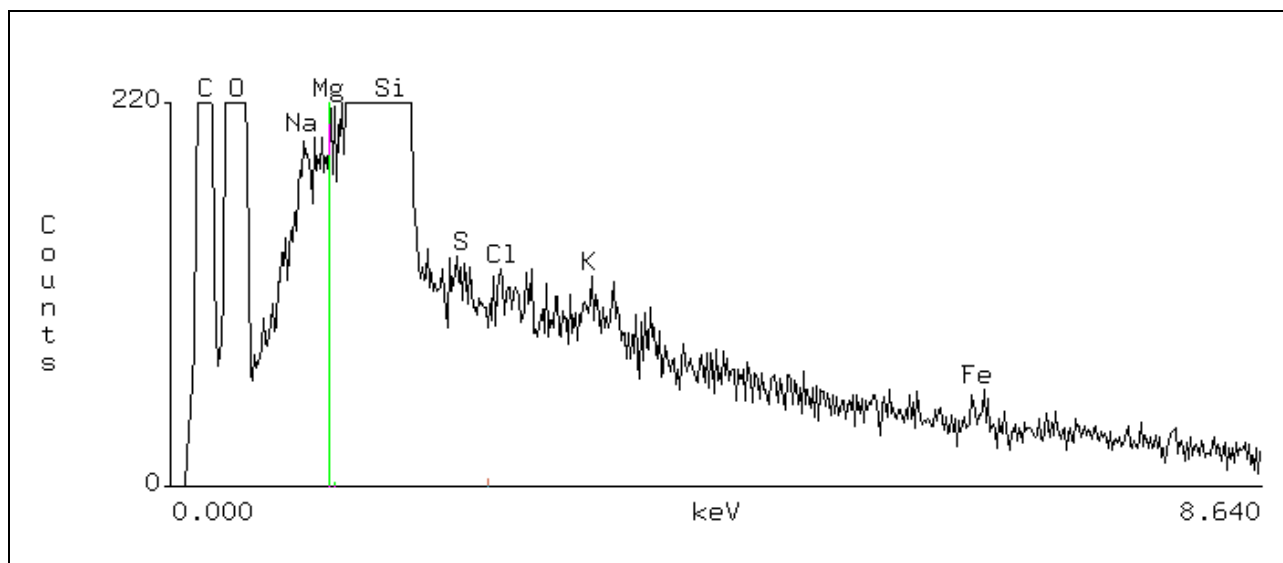


Figure 16. EDX (Element Dispersion X-ray) profile obtained in SEM. Analyses of a 0.2 * 0.2 mm area of quartz. Note the traces of Fe, K, Na, Cl and S. The peaks at Fe and CL are thought to originate from the discolouring of the sample, whereas K, Na seem to originate from some feldspar contamination of the quartz at its surface. S is interpreted to originate from the air (automobile combustion).

Table 1. Kina1: Chlorite composition; calculation of number of cations on the basis of 24 oxygens

Chlorite Kina-1

Element	k-ratio (calc.)	ZAF	Atom %	Element Wt %	Wt % Err. (1-Sigma)	Compound Formula	Compound Wt %	No. of Cations
Mg-K	0.0401	2.052	7.87	8.23	+/- 0.07	MgO	13.65	3.127
Al-K	0.0587	1.827	9.23	10.72	+/- 0.08	Al2O3	20.25	3.669
Si-K	0.0864	1.634	11.69	14.12	+/- 0.09	SiO2	30.22	4.645
K -K	0.0097	1.169	0.67	1.13	+/- 0.03	K2O	1.36	0.267
Ti-K	0.0024	1.155	0.13	0.28	+/- 0.03	TiO2	0.46	0.053
Fe-K	0.1941	1.175	9.49	22.80	+/- 0.18	Fe2O3	32.60	3.772
Na-K	0.0001	2.983	0.04	0.04	+/- 0.03	Na2O	0.06	0.017
Cl-K	0.0005	1.316	0.05	0.07	+/- 0.02	Cl	0.07	0.019
Mn-K	0.0086	1.198	0.44	1.03	+/- 0.05	MnO	1.33	0.174
O -K	---	2.084	60.39	41.57 S	---	---	---	---
Total			100.00	100.00			100.00	15.742

Chlorite Kina1-2

Element	k-ratio (calc.)	ZAF	Atom %	Element Wt %	Wt % Err. (1-Sigma)	Compound Formula	Compound Wt %	No. of Cations
Na-K	0.0016	2.745	0.42	0.43	+/- 0.04	Na2O	0.58	0.168
Mg-K	0.0573	1.932	10.19	11.07	+/- 0.08	MgO	18.35	4.082
Al-K	0.0670	1.816	10.10	12.17	+/- 0.08	Al2O3	22.99	4.042
Si-K	0.0886	1.657	11.70	14.68	+/- 0.09	SiO2	31.41	4.685
Cl-K	0.0012	1.337	0.10	0.17	+/- 0.02	Cl	0.17	0.042
K -K	0.0020	1.186	0.14	0.24	+/- 0.02	K2O	0.29	0.056
Ca-K	0.0015	1.122	0.09	0.17	+/- 0.02	CaO	0.23	0.037
Mn-K	0.0060	1.210	0.30	0.73	+/- 0.05	MnO	0.94	0.118
Fe-K	0.1475	1.187	7.02	17.51	+/- 0.15	Fe2O3	25.04	2.811
O -K	---	2.072	59.94	42.84 S	---	---	---	---
Total			100.00	100.00			100.00	16.042

Chlorite Kina1-3

Element	k-ratio (calc.)	ZAF	Atom %	Element Wt %	Wt % Err. (1-Sigma)	Compound Formula	Compound Wt %	No. of Cations
Mg-K	0.0447	2.032	8.59	9.07	+/- 0.07	MgO	15.04	3.422
Al-K	0.0641	1.834	10.02	11.75	+/- 0.08	Al2O3	22.21	3.993
Si-K	0.0822	1.657	11.16	13.62	+/- 0.09	SiO2	29.13	4.445
K -K	0.0015	1.173	0.11	0.18	+/- 0.02	K2O	0.22	0.042
Ti-K	0.0000	1.131	0.00	0.00	+/- 0.02	TiO2	0.00	0.001
Fe-K	0.1881	1.177	9.12	22.14	+/- 0.17	Fe2O3	31.65	3.634
Na-K	0.0011	2.931	0.33	0.33	+/- 0.03	Na2O	0.44	0.131
Cl-K	0.0005	1.323	0.05	0.07	+/- 0.02	Cl	0.07	0.019
Mn-K	0.0080	1.199	0.40	0.95	+/- 0.05	MnO	1.23	0.159
O -K	---	1.976	60.23	41.88 S	---	---	---	---
Total			100.00	100.00			100.00	15.846

Chlorite Kina1-4

Element	k-ratio (calc.)	ZAF	Atom %	Element Wt %	Wt % Err. (1-Sigma)	Compound Formula	Compound Wt %	No. of Cations
Mg-K	0.0406	2.071	8.03	8.42	+/- 0.08	MgO	13.96	3.193
Al-K	0.0616	1.844	9.76	11.35	+/- 0.09	Al2O3	21.45	3.880
Si-K	0.0813	1.656	11.13	13.47	+/- 0.09	SiO2	28.82	4.422
Fe-K	0.2080	1.174	10.15	24.42	+/- 0.20	Fe2O3	34.92	4.032
K -K	0.0025	1.171	0.17	0.29	+/- 0.03	K2O	0.35	0.069
Na-K	0.0010	3.004	0.29	0.29	+/- 0.04	Na2O	0.39	0.117

Cl-K	0.0008	1.320	0.07	0.11	+/- 0.02	Cl	0.11	0.028
O -K	---	1.977	60.39	41.64	S ---	---	---	---
Total			100.00	100.00			100.00	15.742

Table 2. *Kina1: Biotite composition; calculation of number of cations on the basis of 24 oxygens*

Biotite Kina1-1

Element	k-ratio (calc.)	ZAF	Atom %	Element Wt %	Wt % Err. (1-Sigma)	Compound Formula	Compound Wt %	No. of Cations
Mg-K	0.0298	1.913	5.35	5.70	+/- 0.06	MgO	9.45	2.135
Al-K	0.0601	1.683	8.55	10.12	+/- 0.07	Al2O3	19.12	3.414
Si-K	0.1173	1.536	14.64	18.02	+/- 0.09	SiO2	38.55	5.842
K -K	0.0636	1.175	4.36	7.47	+/- 0.06	K2O	9.00	1.740
Ti-K	0.0118	1.195	0.67	1.41	+/- 0.04	TiO2	2.34	0.267
Fe-K	0.1221	1.191	5.94	14.55	+/- 0.13	Fe2O3	20.80	2.372
Na-K	0.0007	2.732	0.20	0.20	+/- 0.03	Na2O	0.27	0.079
Cl-K	0.0001	1.310	0.01	0.01	+/- 0.02	Cl	0.01	0.003
Mn-K	0.0029	1.217	0.15	0.35	+/- 0.04	MnO	0.45	0.058
O -K	---	2.931	60.14	42.17	S ---	---	---	---
Total			100.00	100.00			100.00	15.910

Biotite Kina1-2

Element	k-ratio (calc.)	ZAF	Atom %	Element Wt %	Wt % Err. (1-Sigma)	Compound Formula	Compound Wt %	No. of Cations
Mg-K	0.0276	1.953	5.14	5.39	+/- 0.06	MgO	8.93	2.056
Al-K	0.0544	1.699	7.94	9.24	+/- 0.07	Al2O3	17.46	3.178
Si-K	0.1122	1.530	14.18	17.17	+/- 0.09	SiO2	36.73	5.673
K -K	0.0677	1.167	4.69	7.91	+/- 0.06	K2O	9.52	1.877
Ti-K	0.0168	1.188	0.97	1.99	+/- 0.04	TiO2	3.32	0.386
Fe-K	0.1354	1.187	6.68	16.07	+/- 0.14	Fe2O3	22.97	2.670
Cl-K	0.0015	1.299	0.13	0.19	+/- 0.02	Cl	0.19	0.051
Mn-K	0.0055	1.212	0.28	0.67	+/- 0.04	MnO	0.87	0.113
O -K	---	2.991	59.99	41.37	S ---	---	---	---
Total			100.00	100.00			100.00	16.006

Biotite Kina1-3

Element	k-ratio (calc.)	ZAF	Atom %	Element Wt %	Wt % Err. (1-Sigma)	Compound Formula	Compound Wt %	No. of Cations
Mg-K	0.0270	1.981	5.13	5.35	+/- 0.06	MgO	8.87	2.072
Al-K	0.0493	1.716	7.30	8.45	+/- 0.07	Al2O3	15.97	2.952
Si-K	0.1100	1.529	13.96	16.82	+/- 0.10	SiO2	35.98	5.641
Fe-K	0.1424	1.186	7.05	16.89	+/- 0.17	Fe2O3	24.15	2.850
K -K	0.0732	1.166	5.09	8.53	+/- 0.08	K2O	10.28	2.055
Na-K	0.0031	2.823	0.90	0.89	+/- 0.04	Na2O	1.19	0.363
Cl-K	0.0034	1.295	0.29	0.44	+/- 0.03	Cl	0.44	0.116
Ti-K	0.0157	1.189	0.91	1.87	+/- 0.05	TiO2	3.12	0.368
O -K	---	3.051	59.38	40.76	S ---	---	---	---
Total			100.00	100.00			100.00	16.416

Table 3. *Kina1: Feldspar composition; calculation of number of cations on the basis of 24 oxygens*

Feldspar_Kina1-1

Element	k-ratio (calc.)	ZAF	Atom %	Element Wt %	Wt % (1-Sigma)	Err. Formula	Compound Wt %	Compound	No. of Cations
Na-K	0.0025	2.254	0.53	0.57	+/- 0.03	Na2O	0.77		0.206
Al-K	0.0729	1.405	8.10	10.24	+/- 0.06	Al2O3	19.35		3.151
Si-K	0.2198	1.372	22.91	30.16	+/- 0.13	SiO2	64.51		8.917
K -K	0.1014	1.213	6.71	12.30	+/- 0.08	K2O	14.82		2.613
Ba-L	0.0034	1.471	0.08	0.50	+/- 0.06	BaO	0.55		0.030
O -K	---	3.567	61.67	46.24	S	---	---	---	---
Total			100.00	100.00			100.00		14.917

Feldspar Kina1-2

Element	k-ratio (calc.)	ZAF	Atom %	Element Wt %	Wt % (1-Sigma)	Err. Formula	Compound Wt %	Compound	No. of Cations
Al-K	0.0703	1.400	7.77	9.83	+/- 0.06	Al2O3	18.58		3.033
Si-K	0.2223	1.362	22.99	30.27	+/- 0.13	SiO2	64.76		8.971
K -K	0.1088	1.212	7.19	13.19	+/- 0.09	K2O	15.89		2.807
Na-K	0.0026	2.249	0.54	0.58	+/- 0.03	Na2O	0.78		0.210
O -K	---	3.649	61.51	46.13	S	---	---	---	---
Total			100.00	100.00			100.00		15.021

Granite panel without discolouring: Kina2

Macroscopic description:

The rock is medium to coarse grained (grain size between 1 and 4 mm) and shows a igneous texture with no noticeable preferred orientation of minerals (Fig. 17).

Microscopic description:

The general appearance of the thinsections which were cut at different orientation to the surface and fabric are shown in Figure 18. These show no preferred orientation of biotite and chlorite in any direction.

The rock is coarse grained and exhibits an igneous texture (Figure 19). The main constituents of the rock are quartz, feldspar and biotite, accessories are chlorite, magnetite and muscovite. Chlorite replaces in places partly or completely biotite (for details see below) and it is frequently associated with magnetite. Magnetite crystals (0.1 – 0.5 mm) are idiomorphic and often associated with biotite and chlorite. Feldspar (up to 4 mm) is characterized by a chemical zonation from core to rim which is typical for feldspars of igneous origin. In addition, sericite and muscovite laths which are aligned along crystallographic planes are abundant in the core of the feldspar crystals. The rock does not exhibit a preferred orientations of the biotite (< 2 mm), feldspar and chlorite laths (Fig. 20) in any way (Fig. 17).



Figure 17. *Cut-out handspecimen of sample Kina2, granite from Kongens Nytorv Metro Station. Note there is no discolouration seen on the top surface and there is no obvious preferred orientation of biotite or feldspars laths in the rock.*



Figure 18. Scans of the 3 different thinsections made from sample Kina2. Note that there is no shape preferred orientation of biotite and that the crystals are coarse grained. For orientation of thinsections see Figure 2. Length of slides ca. 5 cm

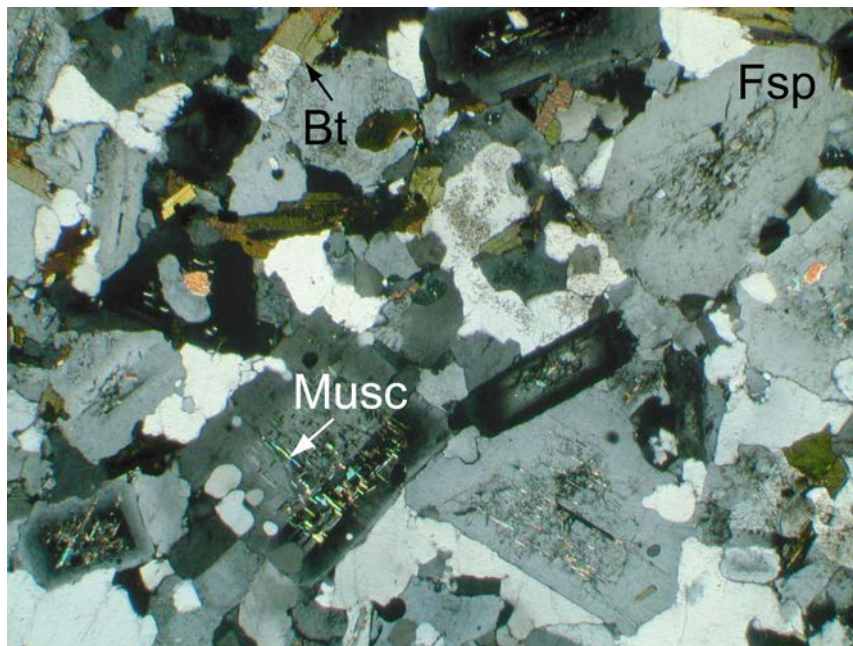


Figure 19. General appearance of Kina2 (thinsection Kina2-3) under the microscope. The igneous feldspar shows a well developed chemical zonation from core to rim and sericite/muscovite laths in the core. Quartz shows no undulatory extinction pointing to no noticeable deformation after crystallization. Grain boundaries are slightly curved to straight. Micrograph is taken with crossed nicols and width of view is 7 mm.

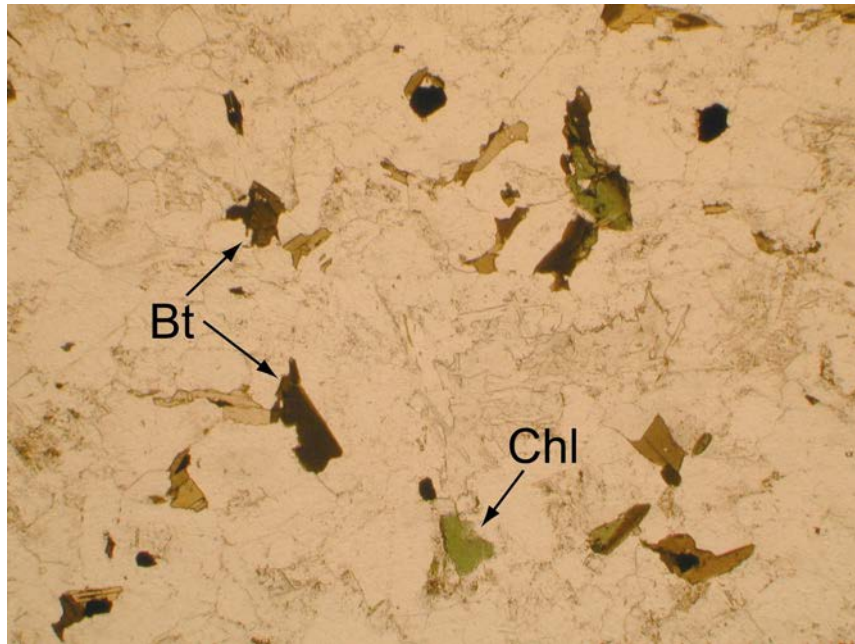


Figure 20. *Photomicrograph showing the random orientation of biotite and chlorite seen in Kina2 (thinsection Kina2-3). Note also the partial to complete replacement of biotite by chlorite. Micrograph is taken in plain light and width of view is 7 mm.*

Scanning electron microscope investigations

SEM investigations show that chlorite replaces to some extent biotite in several instances (Fig. 21 and Fig. 23). The crystallographic basal $\langle a \rangle$ planes of biotite are well seen in the SE and BSE images (Fig. 23). Chlorite has a relatively smooth surface appearance with some minor pits (Fig. 23). The surface of feldspars and inclosed muscovite and sericite are generally smooth (Fig. 24 and Fig. 25). Magnetite shows idiomorphic shapes and the surface of it is characterised by concave, shallow, bowl-shaped ditches (Fig. 22). Grain boundaries in the vicinity of chlorite and biotite aggregates are visible in the SE images but not very pronounced. They are characterized by small pits (Fig. 24).

Examples of the composition of chlorite, biotite and feldspar are given in Tab. 4, 5 and 6. Biotite and chlorite are Fe-rich and show some traces of Cl^- which replaces the OH^- groups in these minerals. The feldspars are generally of albitic to kalifeldspatic composition. The element spectrum obtained from a quartz shows not only a Si peak but also traces of S, Na, K. Only minor traces (if any) of Fe and Cl are seen (Fig. 26).

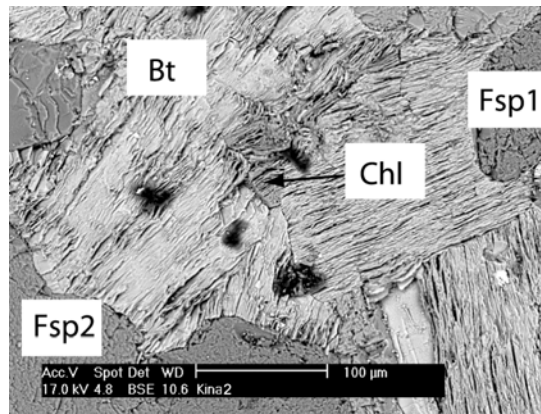


Figure 21. *Biotite with minor replacement chlorite; BSE image*

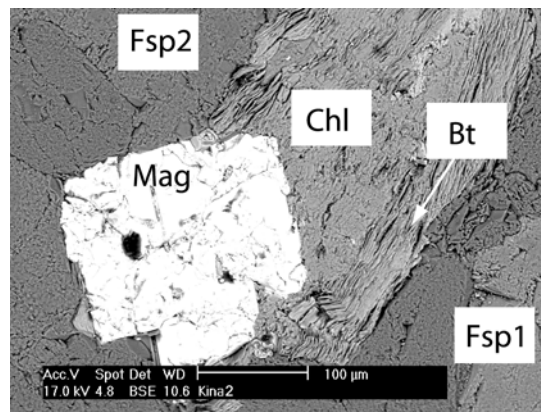


Figure 22. *Biotite-chlorite aggregate next to a magnetite crystal; BSE image.*

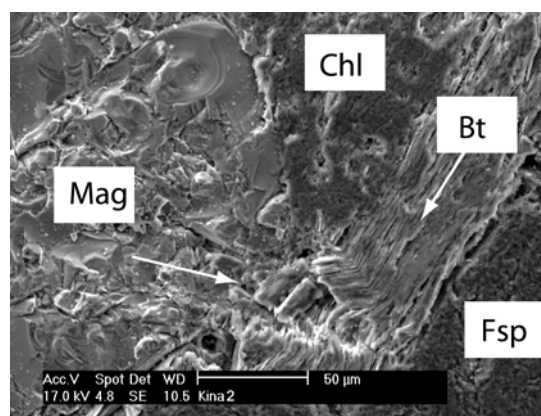


Figure 23. *Close-up of same location as Fig. 22; in a SE image. Note that the cleavage of biotite gives a high surface-ditch appearance to the biotite. The chlorite shows no profound irregular surface; in contrast it appears rather smooth. The magnetite shows a irregular surface with characteristic bowl-shaped structures.*

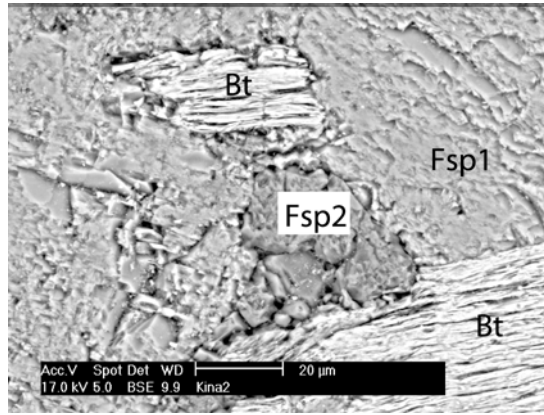


Figure 24. *Biotite crystals imbedded in feldspar; BSE image. Note the feldspar boundaries seen in the image (different gray-scales).*

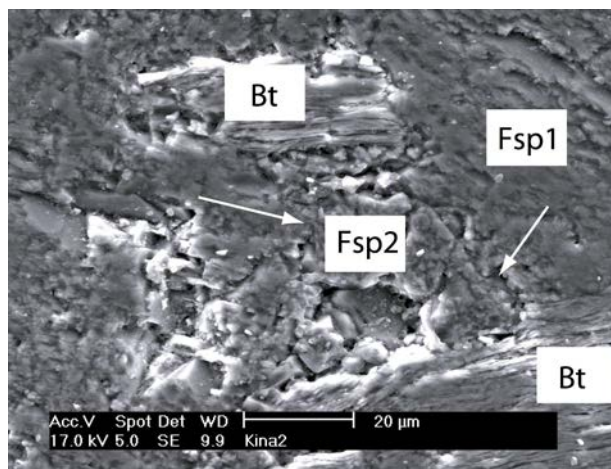


Figure 25. *Same as Fig. 24; SE image. Note the feldspar boundaries are not well pronounced in the type of image (arrows). They are characterized by only minor indentations in the surface.*

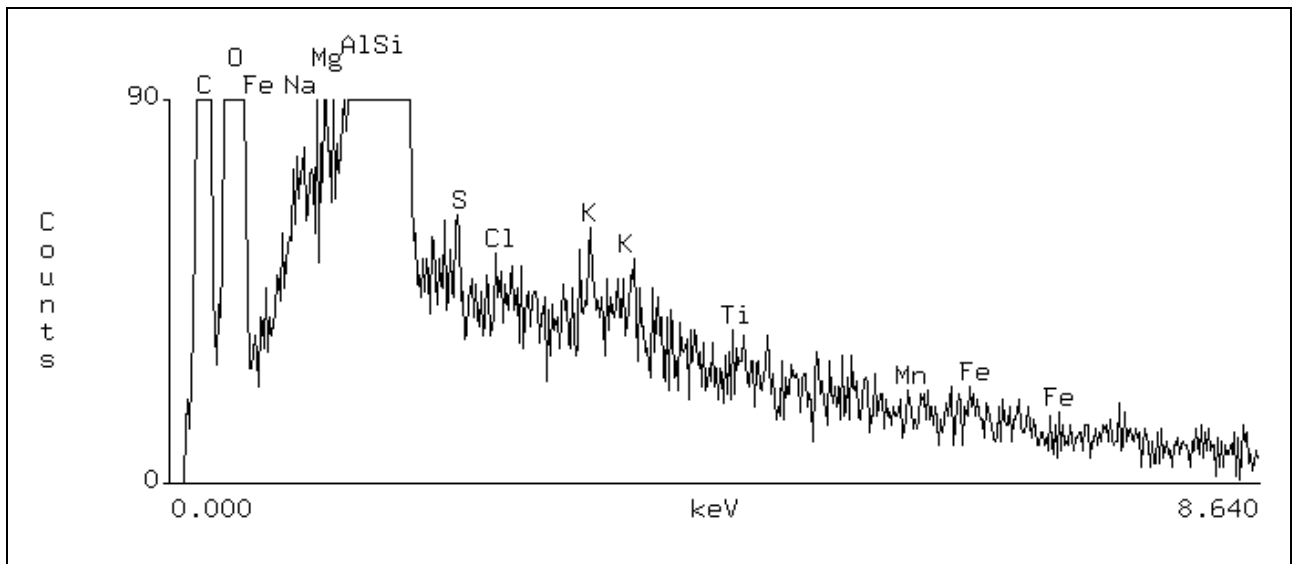


Figure 26. EDX profile obtained in SEM. Analyses of a 0.2 * 0.2 mm area of quartz in the Kina2 sample. Note the traces of K and Na and S, but only very minor if any peaks for Cl and Fe.

Table 4. Kina2: Chlorite composition; calculation of number of cations on the basis of 24 oxygens

Chlorite Kina2-1

Element	k-ratio (calc.)	ZAF	Atom %	Element Wt %	Wt % Err. (1-Sigma)	Compound Formula	Compound Wt %	No. of Cations
Mg-K	0.0412	2.074	8.20	8.55	+/- 0.08	MgO	14.18	3.259
Al-K	0.0598	1.848	9.54	11.05	+/- 0.08	Al2O3	20.87	3.793
Si-K	0.0800	1.652	10.96	13.21	+/- 0.09	SiO2	28.27	4.358
Cl-K	0.0011	1.315	0.09	0.14	+/- 0.02	Cl	0.14	0.036
K -K	0.0021	1.169	0.15	0.25	+/- 0.03	K2O	0.30	0.058
Ti-K	0.0004	1.149	0.02	0.05	+/- 0.03	TiO2	0.09	0.010
Fe-K	0.2142	1.173	10.48	25.12	+/- 0.20	Fe2O3	35.91	4.167
Na-K	0.0006	3.014	0.18	0.18	+/- 0.04	Na2O	0.24	0.072
O -K	---	1.961	60.37	41.45 S	---	---	---	---
Total			100.00	100.00			100.00	15.754

Table 5. Kina2: Biotite composition; calculation of number of cations on the basis of 24 oxygens

Biotite Kina2-1

Element	k-ratio (calc.)	ZAF	Atom %	Element Wt %	Wt % Err. (1-Sigma)	Compound Formula	Compound Wt %	No. of Cations
Mg-K	0.0238	1.987	4.55	4.73	+/- 0.05	MgO	7.84	1.819
Al-K	0.0523	1.706	7.73	8.92	+/- 0.07	Al2O3	16.86	3.093
Si-K	0.1112	1.529	14.15	17.00	+/- 0.09	SiO2	36.36	5.661
K -K	0.0705	1.164	4.90	8.20	+/- 0.07	K2O	9.88	1.962
Ti-K	0.0153	1.185	0.89	1.82	+/- 0.04	TiO2	3.03	0.355
Fe-K	0.1479	1.185	7.33	17.52	+/- 0.15	Fe2O3	25.05	2.934
Na-K	0.0008	2.865	0.24	0.23	+/- 0.03	Na2O	0.31	0.095
Cl-K	0.0006	1.296	0.05	0.08	+/- 0.02	Cl	0.08	0.021
Mn-K	0.0038	1.210	0.20	0.46	+/- 0.04	MnO	0.59	0.078
O -K	---	2.975	59.97	41.05 S	---	---	---	---
Total			100.00	100.00			100.00	16.018

Biotite Kina2-2

Element	k-ratio (calc.)	ZAF	Atom %	Element Wt %	Wt % Err. (1-Sigma)	Compound Formula	Compound Wt %	No. of Cations
Mg-K	0.0288	1.962	5.40	5.65	+/- 0.06	MgO	9.37	2.169
Al-K	0.0512	1.711	7.55	8.76	+/- 0.07	Al2O3	16.55	3.029
Si-K	0.1110	1.529	14.05	16.98	+/- 0.10	SiO2	36.33	5.641
Cl-K	0.0005	1.297	0.04	0.07	+/- 0.02	Cl	0.07	0.017
K -K	0.0709	1.166	4.91	8.26	+/- 0.07	K2O	9.95	1.972
Ti-K	0.0146	1.188	0.84	1.74	+/- 0.05	TiO2	2.90	0.339
Fe-K	0.1439	1.187	7.10	17.07	+/- 0.16	Fe2O3	24.40	2.852
Na-K	0.0011	2.816	0.31	0.31	+/- 0.03	Na2O	0.42	0.126
O -K	---	2.979	59.78	41.16 S	---	---	---	---
Total			100.00	100.00			100.00	16.145

Table 6. Kina2: Feldspar composition; calculation of number of cations on the basis of 24 oxygens

Feldspar Kina2-1

Element	k-ratio (calc.)	ZAF	Atom %	Element Wt %	Wt % Err. (1-Sigma)	Compound Formula	Compound Wt %	No. of Cations
Na-K	0.0034	2.246	0.71	0.76	+/- 0.03	Na2O	1.03	0.277
Al-K	0.0706	1.402	7.84	9.90	+/- 0.07	Al2O3	18.71	3.071
Si-K	0.2191	1.363	22.73	29.86	+/- 0.14	SiO2	63.89	8.900
K -K	0.1123	1.211	7.43	13.59	+/- 0.10	K2O	16.38	2.910
O -K	---	3.683	61.29	45.88 S	---	---	---	---
Total			100.00	100.00			100.00	15.158

Feldspar Kina2-2

Element	k-ratio (calc.)	ZAF	Atom %	Element Wt %	Wt % Err. (1-Sigma)	Compound Formula	Compound Wt %	No. of Cations
Na-K	0.0301	2.153	5.77	6.47	+/- 0.06	Na2O	8.72	2.252
Al-K	0.0853	1.471	9.53	12.55	+/- 0.07	Al2O3	23.71	3.721
Si-K	0.1996	1.455	21.19	29.03	+/- 0.13	SiO2	62.11	8.270
Ca-K	0.0305	1.170	1.82	3.57	+/- 0.05	CaO	4.99	0.712
K -K	0.0032	1.225	0.21	0.39	+/- 0.02	K2O	0.47	0.080
O -K	---	2.866	61.48	47.99 S	---	---	---	---
Total			100.00	100.00			100.00	15.036

Granite from Frederiksberg Metro Station

Macroscopic description:

The rock is fine to medium grained (grain size mostly between 0.2 and 2 mm) and shows an igneous texture with a strong fabric which is defined by biotite and chlorite. Both a foliation and lineation is present (Fig. 27).

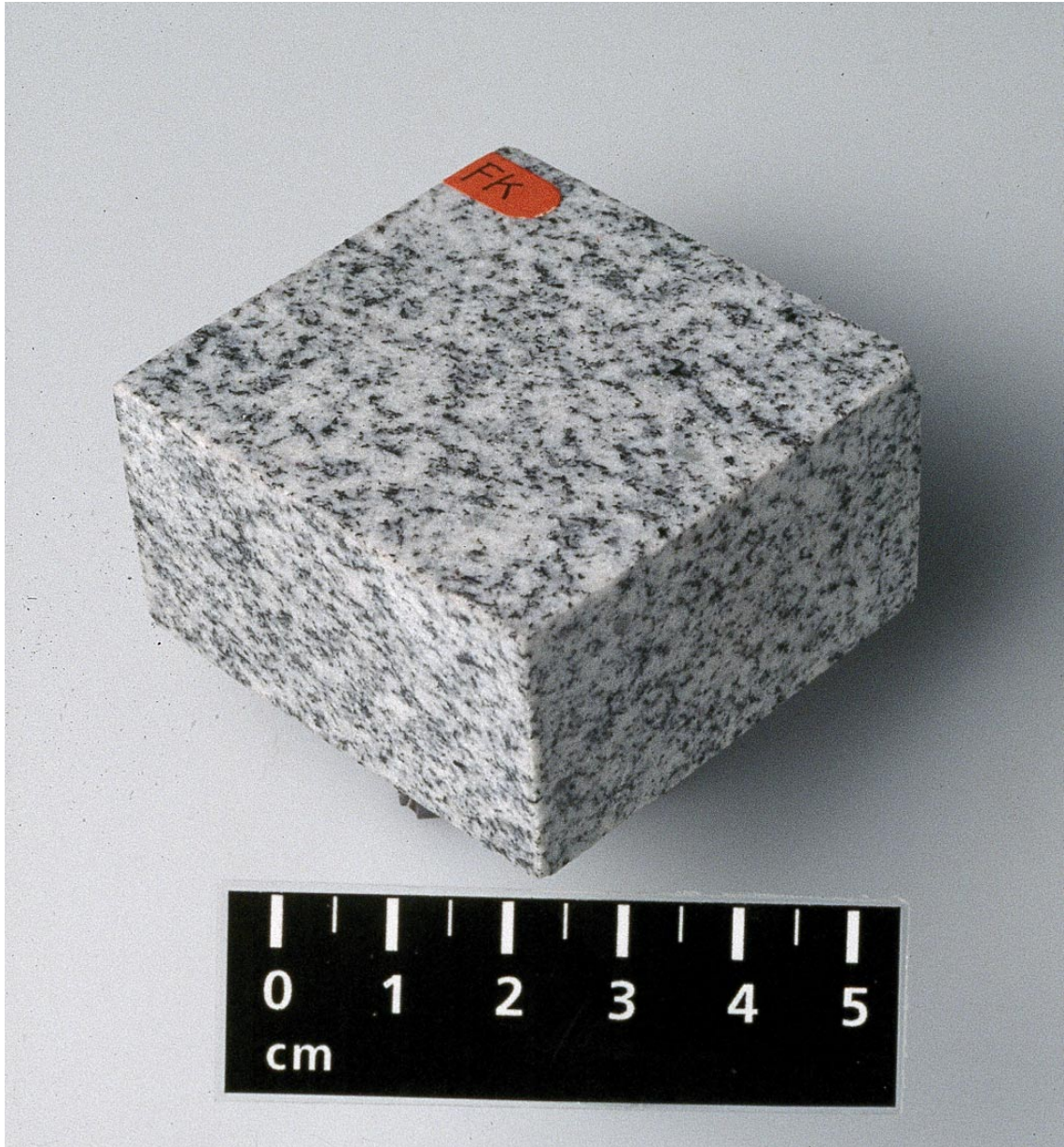


Figure 27. Cut-out handspecimen of sample FK., granite from the Frederiksberg Metro Station. Note the foliated and lineated appearance of the rock.

Microscopic description:

The general appearance of the thinsections which were cut at different orientation to the surface and fabric are shown in Fig. 28. These show a preferred orientation of biotite and chlorite in thinsection FK-1 and FK-3.

The rock is fine to medium grained (grain size between 0.2 and 2 mm) and exhibits an igneous texture (Figure 29b). The main constituents of the rock are quartz, feldspar and biotite, accessories are chlorite, magnetite and muscovite. Chlorite is frequently associated with magnetite or in places partly to completely replaces biotite. Magnetite crystals (0.1 – 0.5 mm) are idiomorphic and often associated with biotite and chlorite. Feldspar (up to 2 mm) is characterized by a chemical zonation from core to rim which is typical for feldspars of igneous origin. In addition, sericite and muscovite laths are abundant in the core of the feldspar crystals.

The rock does exhibit a noticeable preferred orientations of the biotite (< 1 mm), feldspar and chlorite laths (Fig. 29, Fig. 30 and Fig. 31), which originates from a synmagmatic alignment of mineral phases. These now make up an igneous foliation and lineation of the rock (Fig. 27).

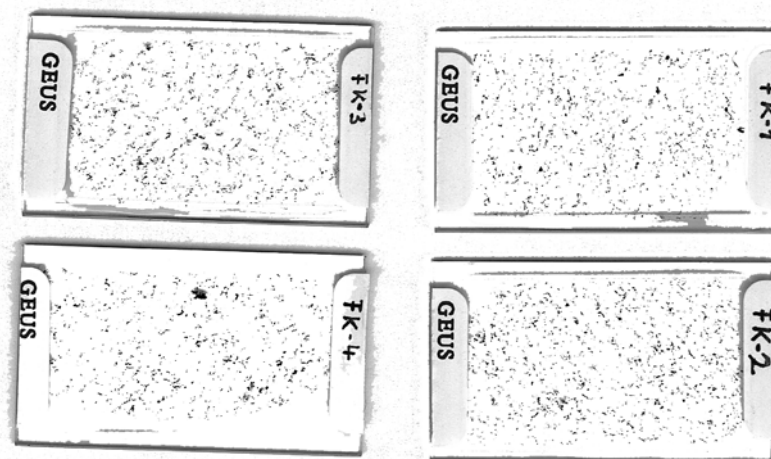


Figure 28. Scans of the 4 different thinsections made from sample FK. Note the shape preferred orientation of predominately small grained biotite in thinsections FK-1 and FK-3. For orientation of thinsections see Figure 2.

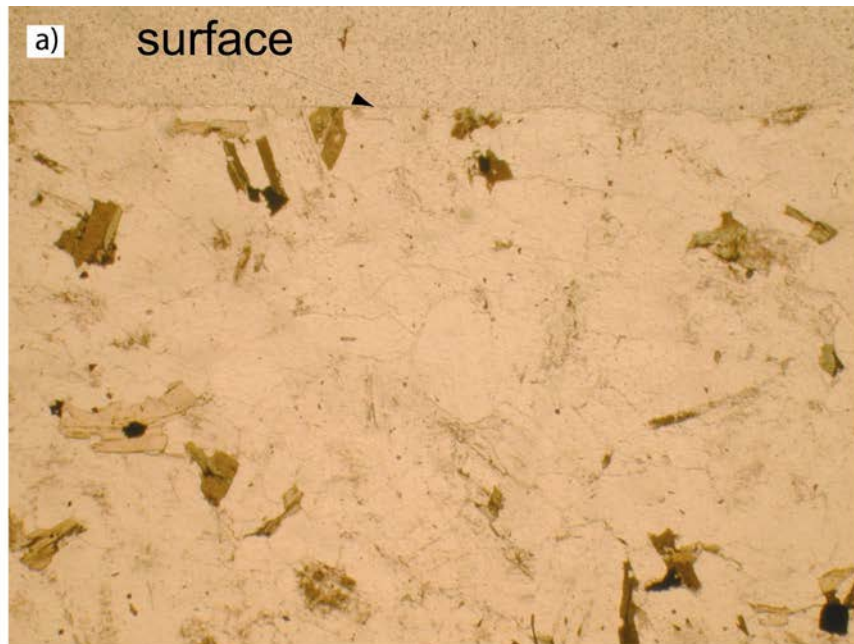


Figure 29. a) Photomicrograph showing the random orientation of biotite and chlorite seen in thinsection FK-3. Note also the partial replacement of biotite by chlorite (upper left corner). Micrograph is taken in plain light and width of view is 6.5 mm.

b) Same view as in a); general appearance of FK (thinsection FK-3) under crossed nicols. The igneous feldspar shows a chemical zonation from core to rim and sericite/muscovite laths in the core. Quartz shows some undulatory extinction pointing to noticeable deformation during and possibly slightly after crystallization. Grain boundaries are slightly curved to straight. Micrograph is taken with crossed nicols and width of view is 6.5 mm.

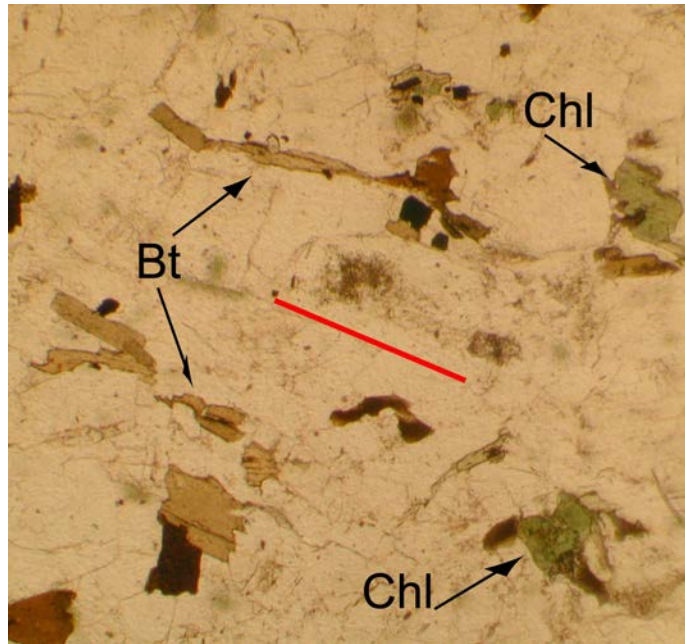


Figure 30. Alignment of biotite and chlorite within FK-2. The red line shows the general orientation of the biotite and chlorite laths. Micrograph is taken in plain light and width of view is 5 mm

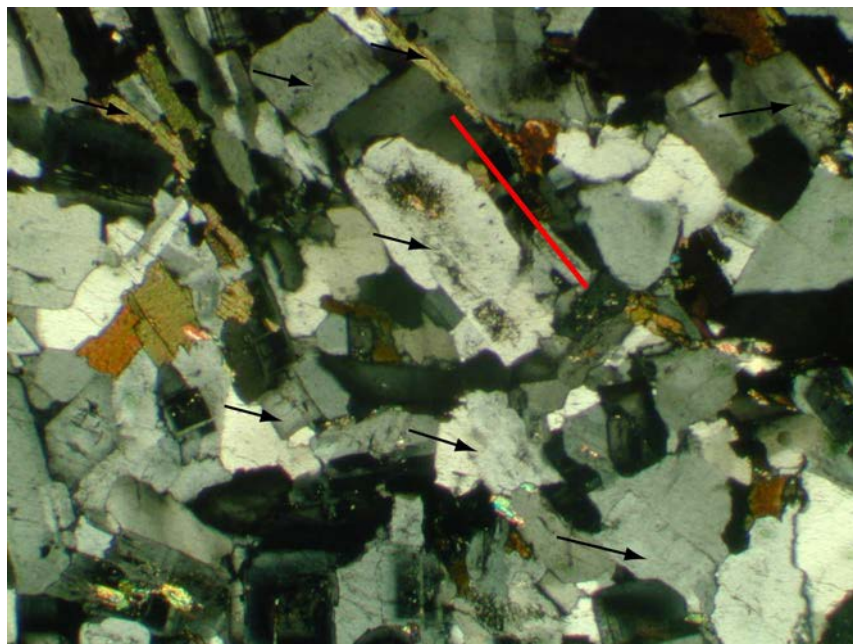


Figure 31. Alignment of feldspar laths and biotite (see arrows) within FK-2. Location partly the same as in Fig. 30 (note long Bt laths). The red line shows the general orientation of the feldspar and biotite laths. Micrograph is taken with crossed nicols and width of view is 5 mm

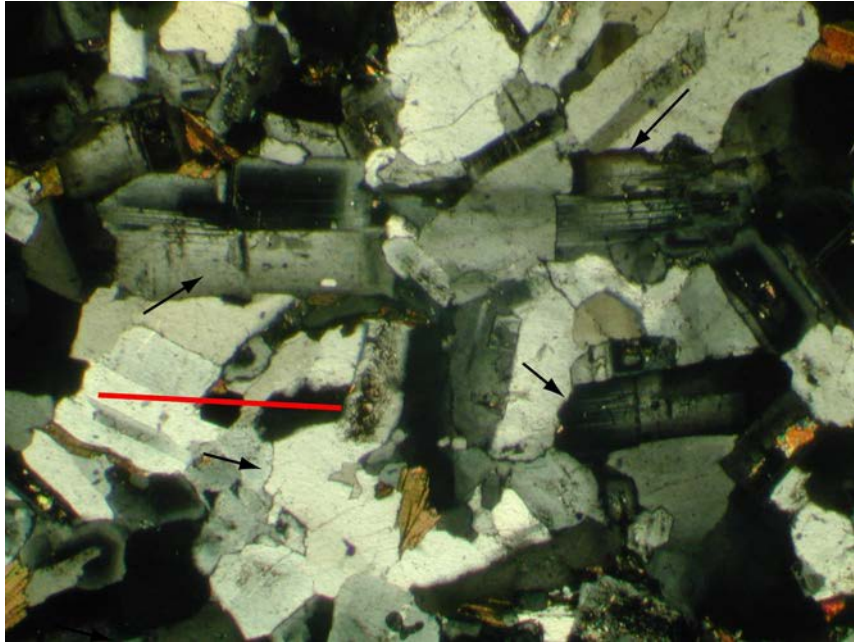


Figure 32. *Alignment of feldspar laths within FK-2. The red line shows the general orientation of the feldspar laths (arrows). Micrograph is taken with crossed nicols and width of view is 5 mm*

Granite from Nørreport Station

Macroscopic description:

The rock is coarse grained (grain size mostly between 1 and 4 mm) and shows a igneous texture with a no preferred orientation of biotite or feldspar laths (Photo D).



Figure 33. *Cut-out handspecimen of sample NP1, granite from Nørreport Metro Station. Note there is no discolouration on the top surface and the igneous, unfoliated and lineated appearance of the rock.*

Microscopic description:

The general appearance of the thinsections which were cut at different orientation to the surface and fabric is shown in Figure 34. These show no preferred orientation of biotite.

The rock is coarse grained and exhibits a well preserved igneous texture (Fig. 35). The main constituents of the rock are quartz, feldspar and biotite, accessories are magnetite, ilmenite, titanite and muscovite. Note that no significant amount of chlorite is present in this rock. Magnetite and ilmenite crystals (0.1 – 0.5 mm) are idiomorphic and often associated with biotite. Feldspar (up to 4 mm) is characterized by its typical appearance for a microcline (cross-hatched twinning) and perthite (flame-like exsolution structures) (cf. Fig. 35). Quartz boundaries are bulging pointing to high temperature grain boundary migration and annealing (Fig. 36). The rock does not exhibit any noticeable preferred orientations of the biotite (< 3 mm) and feldspar.

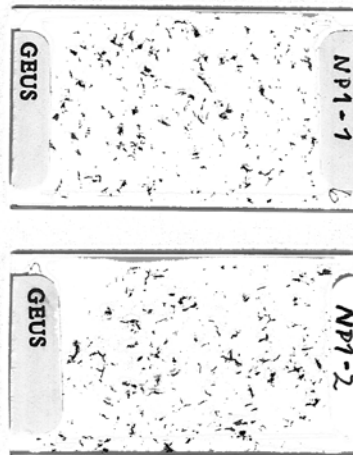


Figure 34. Scans of the 2 perpendicular thinsections made from sample NP1. Note that there is no shape preferred orientation of the coarse grained biotite. For orientation of thinsections see Figure 2.

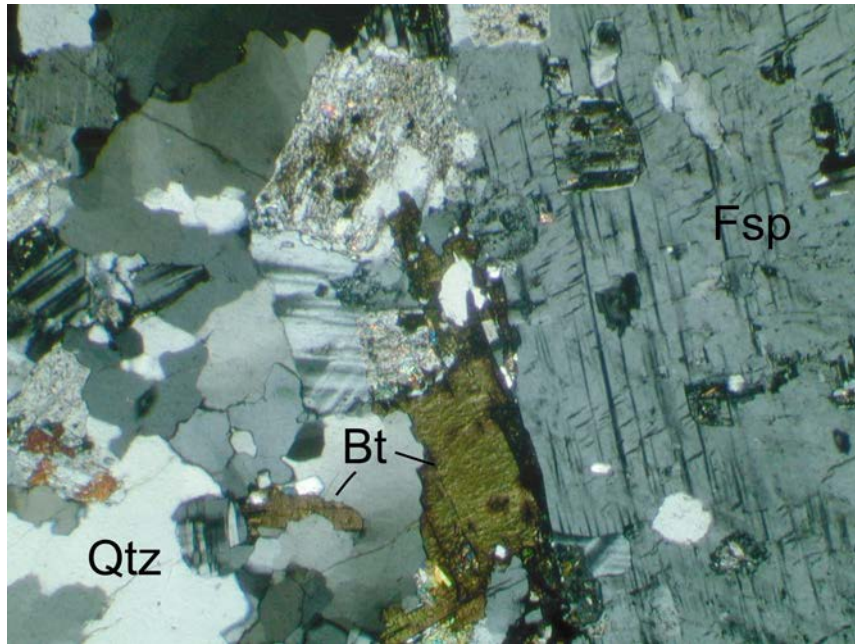


Figure 35. General appearance of NP1 (thinsection NP1-1). The igneous feldspar has a perthitic (right hand side) and cross-hatched microclinal appearance (feldspar just above Bt label). Quartz shows strongly bulging boundaries. Micrograph is taken with crossed nicols and width of view is 6 mm;

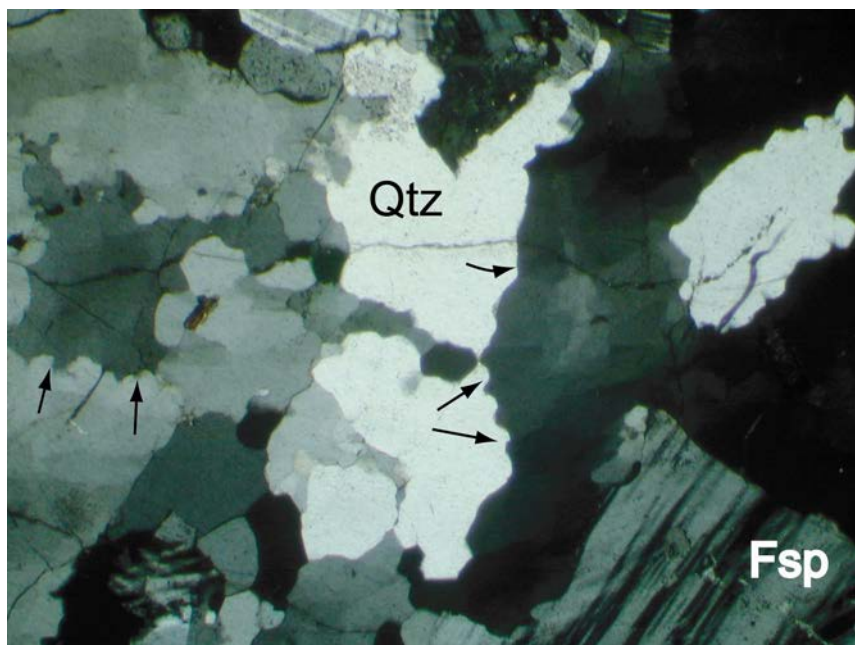


Figure 36. Photomicrograph showing the bulging grain boundaries of quartz which point to high temperature grain boundary migration and annealing. Micrograph is taken in plain light with crossed nicols and width of view is 6 mm.

SEM analyses and description

SEM investigations show that biotite is only rarely replaced by chlorite. The crystallographic basal $\langle a \rangle$ planes of biotite are well seen in the BSE images (Fig. 37). A close-up of the grain boundaries adjacent biotites show no profound surface structure, namely pits. The surface of feldspars are generally smooth (Fig. 37).

Examples of the composition of biotite and feldspar are given in Tab. 2. Biotite and chlorite are Fe-rich and show some traces of Cl. The feldspars are microclines and perthites.

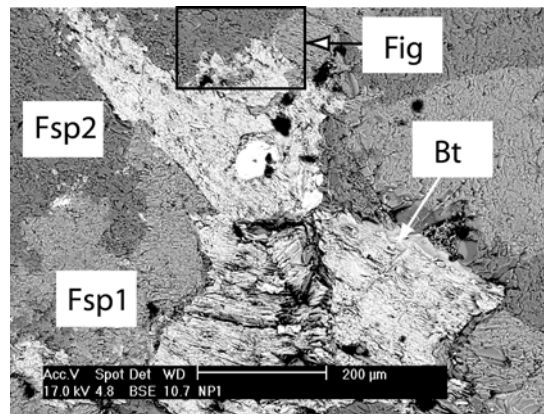


Figure 37. *Biotite without chlorite replacement; BSE image.*

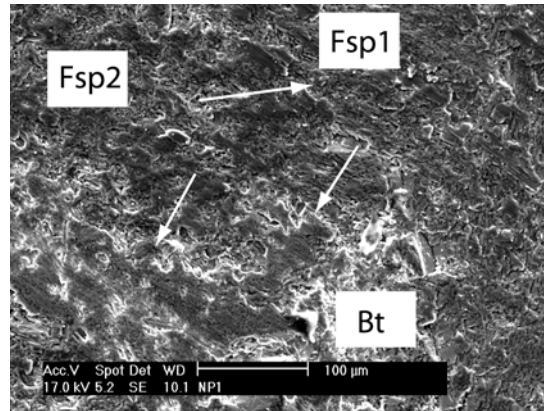


Figure 38. *Close-up of upper middle part of Fig. 37; SE image. Note that the feldspar and biotite grain boundaries are difficult to detect in this image. Boundaries are not marked by ditches or pits.*

Table 7. NP1: Biotite composition; calculation of number of cations on the basis of 24 oxygens

Biotite NP1-1

Element	k-ratio (calc.)	ZAF	Atom %	Element Wt %	Wt % Err. (1-Sigma)	Compound Formula	Compound Wt %	No. of Cations
Mg-K	0.0132	2.049	2.63	2.70	+/- 0.05	MgO	4.47	1.044
Al-K	0.0518	1.701	7.76	8.81	+/- 0.07	Al2O3	16.66	3.076
Si-K	0.1123	1.522	14.44	17.08	+/- 0.10	SiO2	36.55	5.727
K -K	0.0687	1.159	4.83	7.95	+/- 0.07	K2O	9.58	1.915
Ti-K	0.0139	1.176	0.81	1.64	+/- 0.05	TiO2	2.73	0.322
Fe-K	0.1771	1.179	8.88	20.88	+/- 0.19	Fe2O3	29.85	3.520
Cl-K	0.0009	1.291	0.08	0.12	+/- 0.02	Cl	0.12	0.032
Na-K	0.0001	2.988	0.04	0.03	+/- 0.04	Na2O	0.05	0.014
O -K	---	2.888	60.53	40.78 S	---	---	---	---
Total			100.00	100.00			100.00	15.650

Table 8. NP1: Feldspar composition; calculation of number of cations on the basis of 24 oxygens

Feldspar_NP1-1

Element	k-ratio (calc.)	ZAF	Atom %	Element Wt %	Wt % Err. (1-Sigma)	Compound Formula	Compound Wt %	No. of Cations
Na-K	0.0028	2.240	0.59	0.63	+/- 0.03	Na2O	0.85	0.230
Al-K	0.0697	1.398	7.72	9.74	+/- 0.07	Al2O3	18.41	3.023
Si-K	0.2207	1.358	22.82	29.96	+/- 0.14	SiO2	64.09	8.931
Ca-K	0.0008	1.213	0.05	0.10	+/- 0.03	CaO	0.14	0.021
K -K	0.1133	1.209	7.50	13.70	+/- 0.10	K2O	16.51	2.934
O -K	---	3.681	61.32	45.86 S	---	---	---	---
Total			100.00	100.00			100.00	15.140

Feldspar NP1-2

Element	k-ratio (calc.)	ZAF	Atom %	Element Wt %	Wt % Err. (1-Sigma)	Compound Formula	Compound Wt %	No. of Cations
Na-K	0.0315	2.133	5.94	6.71	+/- 0.19	Na2O	9.05	2.302
Al-K	0.0765	1.468	8.46	11.22	+/- 0.19	Al2O3	21.21	3.279
Si-K	0.2180	1.434	22.63	31.26	+/- 0.32	SiO2	66.87	8.774
Ca-K	0.0151	1.174	0.90	1.78	+/- 0.11	CaO	2.48	0.349
K -K	0.0026	1.234	0.17	0.33	+/- 0.06	K2O	0.39	0.066
O -K	---	2.666	61.90	48.71 S	---	---	---	---
Total			100.00	100.00			100.00	14.771

Summary of petrography

In the light of the question what causes the discoloration in some of the granite types, a comparison of the different characteristics of the different types of granites is needed. The differences between granites that exhibit a surface discoloration and granites that do not are (Fig. 1 and 39):

Characteristics of granite with discoloration (Kina1 and FK)

- fine to medium grained
- moderate to strong shape fabric of biotite, chlorite and igneous feldspar
- abundant and small grained biotite and chlorite
- irregular surface structure of chlorite and biotite
- surface irregularities (pits) along grain boundaries
- high Fe and Cl bearing biotite and chlorite

Characteristics of granite without discoloration (Kina2 and NP1)

- coarse grained
- no shape preferred orientation of mineral species
- low amounts of large grained biotite and chlorite
- smooth surface of chlorite (Kina2)
- very low amount of chlorite (NP1)
- no "eroded" grain boundaries next to biotite crystals

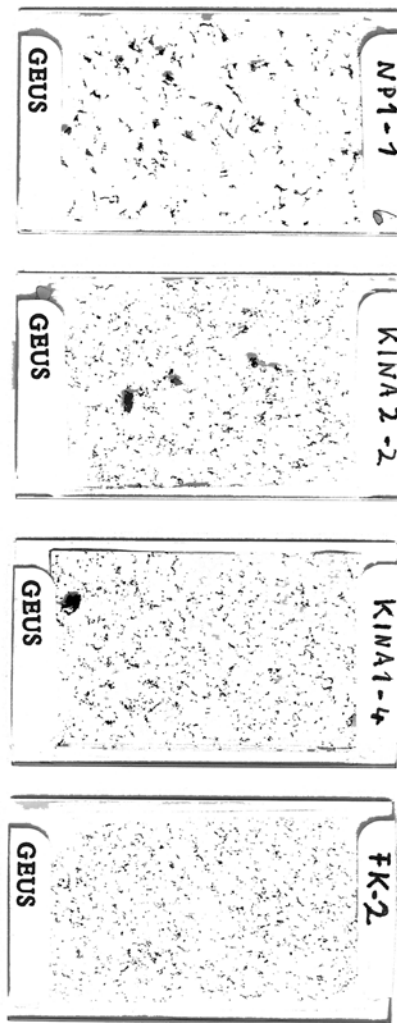


Figure 39. Selected scans of thinsections from discoloured (Kina1 and FK) and not discoloured granites (Kina2 and NP1). Note the difference in alignment, size and amount of mafic minerals (biotite, chlorite, magnetite) in these sections.

Discussion of discolouring of the granite

According to findings summarized above, we suggest that the discolouration of the granites Kina1 and FK originate from the dissolution of Fe-bearing minerals which are biotite, chlorite and magnetite. In our view, the two minerals biotite and chlorite are the most important in this reaction, as they are more abundant than the magnetite and are present in different amounts and different grain sizes in discoloured granites and in non-discoloured granites, Moreover the sheet structured biotite and chlorite show irregular surfaces in the discoloured samples and they contain Cl which could be an agent for further dissolution. Reaction of surface water with these minerals results in dissolution of small amounts of the mineral species. Fe^{2+} from the minerals is oxidatised to Fe^{3+} . This can then built some complexes

with other components present in the fluid e.g. O and Cl and a yellowish staining results. The fact that Cl is also present in the dissolved mineral phase and therefore in the fluid in which the ions of the dissolved matter are present may help to further dissolve the Fe rich phases. Once the reaction starts a positive feedback loop may be the result. Besides the discolouration, an "erosion" along grain boundaries both aids and enhances the described process. In the rocks, which show discolouration, there is a higher amount of grain boundaries per volume than in the non-discoloured samples, as discoloured samples are finer grained than non-discoloured samples. Therefore, in the discoloured samples more surfaces at which the water can "attack" and then dissolve material are available. In addition, the alignment of mineral phases may aid the flow of water along the boundaries and by that further enhance dissolution and therefore permeability of the rock. The higher abundance of mafic minerals in discoloured samples, results in a higher amount of Fe rich material that is available for dissolution altogether. Subsequently, the ferri-dihydroxides are precipitated at the surface as "rust".

Arguments which support this interpretation are:

- the surface of biotite and chlorite in these samples is irregular and shows cavities which point to some dissolution of the material
- the presence of Fe-components on the surface seems to be likely according the tests conducted by BRE (Fig. 4) and SEM element graphs (Fig. 16 and 26)
- the more pronounced discolouration in the vicinity of mafic minerals (biotite, chlorite and magnetite) as shown in Fig. 1 and Fig. 2 in the DMUR report
- grain boundaries are "eroded" in the vicinity of the biotite and chlorite aggregates in the discoloured samples

Porosity and permeability tests of granite tiles

In order to establish the storage and flow properties of the granite tiles, a total of eight 25 mm diameter plug samples were drilled from the Chinese granite and one sample from the Finnish reference granite. The samples were dried and measured for porosity (Table 9). They were next vacuum saturated with tap water for 24 hours and pressure saturated at 1600 psi (~110 bar) for 3 days. The permeability to water was measured during a period of up to 24 hours, see table 10 below. Two massive steel plugs were run as blinds to test the system compressibility and possible leaks. As appears from table 10 the system lower limit of detection is several orders of magnitude below the lowest measured granite permeability.

Sample ID	Orientation	Porosity		Porosity, mean %	Grain density		Grain density, mean g/cc
		1 %	2		1 g/cc	2	
NP1	isotropic	0.71	0.45	0.58	2.643	2.636	2.639
KK1a	hz 1	0.85	0.80	0.82	2.668	2.667	2.668
KK1b	hz 2	1.08	1.14	1.11	2.665	2.667	2.666
KK1c	vert	1.34	1.53	1.43	2.669	2.677	2.673
KK2a	hz 1	1.03	1.02	1.03	2.667	2.667	2.667
KK2b	vert	1.05	1.09	1.07	2.668	2.669	2.669
FKa	hz 1	1.21	1.27	1.24	2.664	2.666	2.665
FKb	hz 2	1.18	1.22	1.20	2.664	2.665	2.665
FKc	vert	1.23	1.29	1.26	2.666	2.668	2.667

Abbr.: hz 1 – horizontal direction 1
 hz 2 – horizontal direction 2
 vert – vertical

Table 9. Copenhagen Metro granite tiles, core analysis data. Porosity and grain density have been measured twice on the samples.

Sample ID	Diameter mm	Length mm	Temp C	Fluid viscosity cP	Cal. flow rate ml/h	Permeability μ D	Hydraulic conductivity E-12 m/s
NP1	24.84	25.88	21	1.00	0.020	0.10	0.97
KK1a	24.81	38.87	21	1.00	0.139	1.05	10.1
KK1b	24.84	9.73	21	1.00	0.461	0.87	8.4
KK1c	24.84	9.24	21	1.00	0.538	0.96	9.3
KK2a	24.88	31.62	21	1.00	0.119	0.72	7.0
KK2b	24.84	36.34	21	1.00	0.067	0.47	4.5
FKa	24.85	39.39	21	1.00	0.273	2.08	20.1
FKb	24.87	39.33	21	1.00	0.206	1.56	15.1
FKc	24.86	30.00	21	1.00	0.176	1.02	9.9
Steel	25.00	25.00	21	1.00	0.0001	0.0005	0.005
Steel	25.00	25.00	21	1.00	0.0002	0.0011	0.011

Table 10. Copenhagen Metro granite tiles, core analysis data. Liquid flow data measured for granite tiles.

Summary of porosity and permeability measurements

The measurements of porosity of the granites show that the porosity in granites from Kongens Nytorv and Frederiksberg, the "Chinese" granites, is twice as high as the porosity of granite from Nørreport, the "Finnish" granite. In the two discoloured samples analysis of porosity in different direction show markedly different values.

The permeability test demonstrates that the Chinese granite has a water permeability roughly 10 times as high compared to the Finnish reference granite. Moreover the permeability varies in different directions, and some of the tiles are thus expected to be more subjected to percolation than others, depending on the orientation of the cut in the granite.

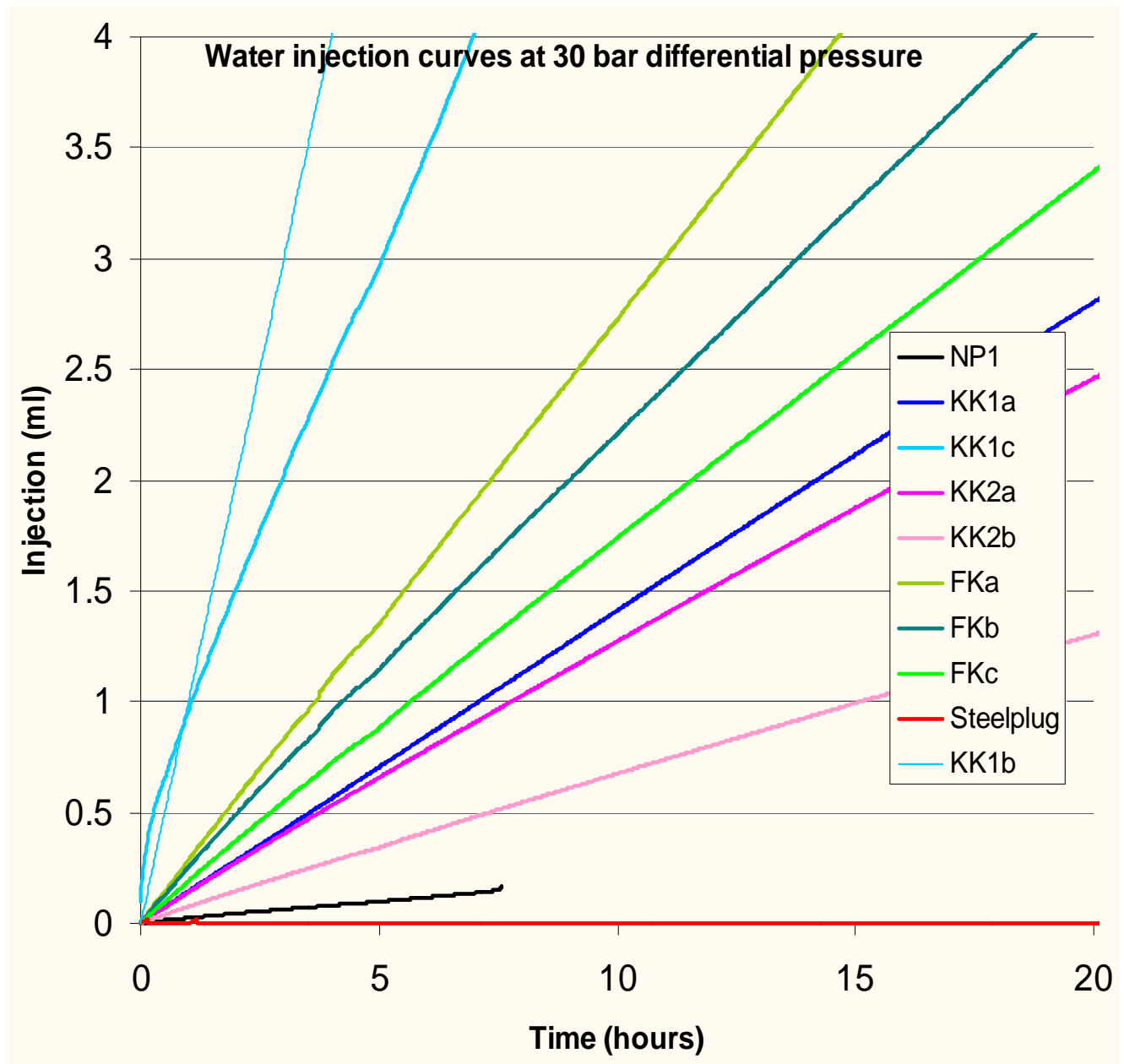


Figure 40. Injection curves recorded by the computer controlled pumping system showing near to ideal flow conditions i.e. constant injection rate throughout experiment. Note that KK1b and KK1c are shorter plugs than the other samples. The blind (steel plug) curve is in essence identical to the x-axis of the diagram.

Analytical Methods

The following is a short description of the methods used by GEUS Core Laboratory. For a more detailed description of methods, instrumentation and principles of calculation the reader is referred to API recommended practice for core-analysis procedure (API RP 40, 2nd ed. 1998).

Sampling

Plugs of diameter 25 mm were drilled from the granite tiles in different directions, horizontal and vertical relative to the lineation. Samples were then dried at 60 °C and analysed for porosity.

He-porosity and grain density

The porosity is measured on dried samples. The porosity is determined by subtraction of the measured grain volume and the measured bulk volume. The Helium technique, employing Boyle's Law, is used for grain volume determination, applying a double chambered Helium porosimeter with digital readout, whereas bulk volume is measured by submersion of the plug in a mercury bath using Archimedes principle. Grain density is calculated from the grain volume measurement and the weight of the dried sample.

Liquid permeability

The water-saturated plug is mounted in a hydrostatic Hassler core holder and a net confining pressure of 50 bar applied to the sleeve. The fluid upstream pressure of 30 bar is delivered from a computer controlled metering pump. Pressures and injected volume are recorded during a period of 24 hours. The liquid permeability is calculated from Darcy's equation for laminar liquid flow in porous media.

Precision of analytical data

The table below gives the precision (= reproducibility) at the 68% level of confidence (+/- 1 standard deviation) for routine core analysis measurements performed at GEUS Core Laboratory.

Measurement	Range, mD	Range, %	Precision
Grain density			0.003 g/cc
Bulk volume (Hg)			0.01 cc
Porosity		< 1 %	0.3 porosity-%
		> 1 %	0.15 porosity-%
Liquid permeability	> E-3		5 %

Discussion of the properties of granites

The two types of granites here investigated show a marked difference in texture and composition. It is obvious that the "Finnish" granite from the Nørreport Station (NP1) has an ordinary granite property, it is coarse grained, homogenous and its texture is isotropic. Additionally, it cannot be penetrated by water (it has a very low permeability typical for granites). It contains a small amount of minerals that could be subject to dissolution and release of iron-compounds which are thought to be responsible for discolouring the surface or grain boundary voids.

The "Chinese" granites used both in the Kongens Nytorv (KK1, KK2) and Frederiksberg Metro station (FK) are predominately medium grained, more inhomogeneous i.e. different tiles show different textures, and the individual tiles have a anisotropic texture (KK1, FK). An anisotropic texture is characterized by a fabric in which minerals are aligned with their long crystallographic axes in one specific, preferred orientation. In several tiles this anisotropy is so pronounced that it can be seen with the naked eye. Permeability tests show clearly that the most permeable tiles are those which exhibit the strongest discoloration.

The source for the discoloration of the "Chinese" granites can be traced back to two main features. First, the higher porosity and permeability rises the capillary effect. The surface in contact with water or air with high humidity will have a tendency of absorbing fluids, which will fill the capillary voids and micro fractures in the granite. This effect will give a dark hue to the granite due to the loss in transparency. When the capillary voids dry out the granite will regain its light colour. However, the capillary absorption and evaporitisation may well result in "pulsing" dissolution and precipitation of volatiles in the granite.

The second element to consider is the yellowish discoloration, which is due to removal of iron from mafic minerals in the granite. The iron is first dissolved from Fe-rich minerals, and then transported to the surface of the granite where it is oxidised and precipitated as ferri-di-hydroxides, in general terms "rust". The investigation of chlorite and biotite in the "Chinese" granites make these two minerals the most favourable candidates for the source of iron. These silicate mineral have a sheet like structure and exhibit high amounts of iron; and the layered, sheeted structure of these mineral species makes it easy for iron to be "washed" off from the mineral surface. The chlorine present within the crystal lattice of biotite and chlorite will furthermore enhance dissolution of iron as a complex-compound suitable for soluble transport. Magnetite is also a mineral with a high content of iron. However, the octahedral structures of magnetite is more compact, and the mineral shows no sign of dissolution at its surface which could be demonstrated in the microscopic analysis.

Conclusion

The discolouring of the granite tiles from the Kongens Nytorv and Frederiksberg Metro Stations is regarded to be the effect of a combination of two phenomenon:

- 1) The capillary penetration of water in the tiles which have a high permeability compared to other granites, exemplified by the granite investigated from the Nørreport Metro Station
- 2) Dissolution of iron from both surfaces of biotite and chlorite in the granite and subsequent precipitation of ferri-dihydroxides at or very near to the exposed surface of the granite.

From the investigation of a discoloured and a non-discoloured granite tile from Kongens Nytorv it is concluded that the permeability of the granites varies a lot with grain size, anisotropy of the texture and structure of the grain boundaries, and thus the discolouring of the tiles will vary considerably.